

High-Energy cosmic-ray antiprotons with the CAPRICE98 experiment

M. Boezio¹, M. Ambriola², S. Bartalucci³, R. Bellotti², D. Bergström⁴, V. Bonvicini¹, U. Bravar⁵, F. Cafagna², P. Carlson⁴, M. Casolino⁶, F. Ciacio², M. Circella², C. N. De Marzo², M. P. De Pascale⁶, N. Finetti⁷, T. Francke⁴, P. Hansen⁴, M. Hof⁸, J. Kremer⁸, W. Menn⁸, J. W. Mitchell⁹, E. Mocchiutti⁴, A. Morselli⁶, J. F. Ormes⁹, P. Papini⁷, S. Piccardi⁷, P. Picozza⁶, M. Ricci³, P. Schiavon¹, M. Simon⁸, R. Sparvoli⁶, P. Spillantini⁷, S. A. Stephens⁹, S. J. Stochaj⁶, R. E. Streitmatter⁹, M. Suffert¹⁰, A. Vacchi¹, E. Vannuccini⁷, and N. Zampa¹

¹University of Trieste and Sezione INFN di Trieste, Trieste, Italy

²University of Bari and Sezione INFN di Bari, Bari, Italy

³INFN – Laboratori Nazionali di Frascati, Frascati, Italy

⁴Royal Institute of Technology, Stockholm, Sweden

⁵R. L. Golden Particle Astrophysics Lab, New Mexico State University, Las Cruces, NM, USA

⁶University of Roma “Tor Vergata” and Sezione INFN di Roma II, Rome, Italy

⁷University of Firenze and Sezione INFN di Firenze, Florence, Italy

⁸University of Siegen, Siegen, Germany

⁹NASA/Goddard Space Flight Center, Greenbelt, MD, USA

¹⁰Centre des Recherches Nucléaires, Strasbourg, France

Abstract. Observations of cosmic-ray antiprotons were performed by the balloon-borne experiment CAPRICE98 that was flown on 28-29 May 1998 from Fort Sumner, New Mexico, USA. The experiment used the NMSU-WIZARD/CAPRICE98 balloon-borne magnet spectrometer equipped with a gas Ring Imaging Cherenkov detector, a time-of-flight system, a tracking device consisting of drift chambers and a superconducting magnet and a silicon-tungsten calorimeter.

We report on the absolute-antiproton-energy spectrum determined in the kinetic energy region at the top of the atmosphere between 3.2 and 49.1 GeV.

references therein). The observed spectrum indicates that the cosmic ray antiprotons are mostly, if not all, produced by the collision of cosmic-ray nuclei with interstellar gas. However, a primary component cannot be excluded.

At energies above 4 GeV only two measurements (Golden et al., 1979; Hof et al., 1996) were performed, prior the CAPRICE98 experiment, and these differ by a large amount. We report here new results on the cosmic-ray antiprotons from 3 to 50 GeV at the top of the atmosphere obtained with the NMSU-WIZARD/CAPRICE98 balloon-borne magnet spectrometer. At these energies, the measurements permit the study of the topics discussed above free of uncertainties associated with the secondary antiproton production and of the uncertainties in the solar modulation effect. Furthermore, it permits us to investigate the possible annihilation of heavy supersymmetric particles (Ullio, 1999).

1 Introduction

The study of antiprotons and positrons is extremely interesting because they provide important information concerning the origin and propagation of cosmic rays in the Galaxy. Moreover, antiprotons can be produced by exotic sources such as evaporation of primordial black holes (Hawking, 1974; Kiraly et al., 1981; Maki et al., 1996) and annihilation of supersymmetric particles (Stecker, Rudaz, & Walsh, 1985; Bottino et al., 1998; Bergström et al., 1999a; Bergström et al., 1999b). The spectrum has been determined quite accurately below 4 GeV kinetic energy (Orito et al, 2000, and

2 The CAPRICE98 apparatus

The balloon-borne CAPRICE98 apparatus was flown on 28-29 May 1998 from Fort Sumner, New Mexico, USA at a vertical rigidity cutoff of about 4.3 GV. It floated at an average atmospheric depth of about 5.5 g/cm² for a period of 21h.

Fig. 1 shows the apparatus (Ambriola et al., 1999). It included from top to bottom: a gas Ring Imaging Cherenkov (RICH) detector, a time-of-flight (ToF) system, a tracking

system consisting of drift chambers and a superconducting magnet and a silicon-tungsten imaging calorimeter.

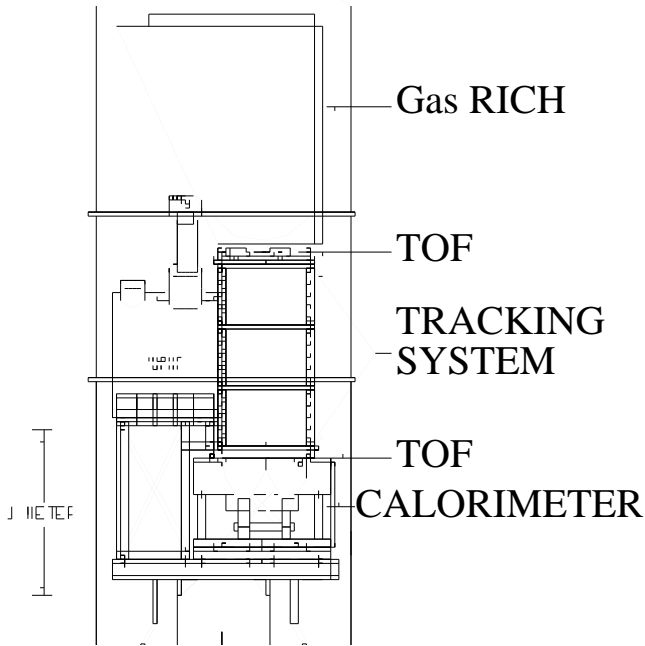


Fig. 1. The CAPRICE98 apparatus in the 1998 configuration (CAPRICE98).

The RICH detector (Francke et al. 1999; Bergström et al. 2001) used a 1 m tall gas radiator filled with high purity C_4F_{10} gas, with an average threshold Lorentz factor of about 19 at float. The Cherenkov light was reflected by a segment of a spherical mirror, located at the bottom of the radiation, onto a photosensitive multiwire proportional chamber with gas readout. The signals were acquired by means of a pad readout implemented on one cathode plane.

The ToF system consisted of two planes of plastic scintillator, located immediately above and below the tracking stack. Each plane was segmented into two paddles viewed at opposite ends by photomultipliers. The signals from each photomultiplier were independently digitized for time-of-flight measurements as well as for ionization losses of the particles. This system reached a time resolution of the order of 200 ps.

The magnet spectrometer had a superconducting magnet and a tracking device. The tracking device consisted of 3 sets of drift chambers (Hof et al., 1994) providing a total of 18 position measurements in the direction of maximum bending, x direction, and 12 along the perpendicular view, y direction, with a resolution better than $100 \mu\text{m}$. The average Maximum Detectable Rigidity of the tracking system was 330 GV for singly charged particles.

The silicon-tungsten calorimeter (Bocciolini et al., 1996) consisted of 8 planes of silicon detectors interleaved with tungsten converters one radiation length thick. Each silicon plane had two layers of sensors segmented in strips along perpendicular directions. The vertical segmentation of the calorimeter and the use of silicon strip detectors provided information on the longitudinal and lateral profiles of the interactions along with a measure of the deposited energy. The calorimeter thickness corresponded to about 0.3 hadronic interaction lengths.

3 Data analysis

The rigidity range of the antiproton analysis was 4 to 50 GV divided in four intervals: 4-8, 8-18, 18-30 and 30-50 GV. The lower limit was due to the geomagnetic cut-off of the experiment, while the upper limit was based on the RICH ability to reliably identify antiprotons from other particles at maximum Cherenkov angle ($\beta \simeq 1$). At 50 GV the (anti)proton Cherenkov angle became less than 3 standard deviations away from the Cherenkov angle of $\beta \simeq 1$ particles.

The primary task of the tracking system was to precisely measure the sign and absolute value of the deflection ($1/\text{rigidity}$) of the particle traversing the apparatus. Events with more than one track, such as products of interactions, were eliminated. For this reason a set of strict selection criteria was imposed on the quality of the fitted tracks. These criteria were based partly on experience gained during the analysis of data from a similar tracking system (Hof et al., 1996; Mitchell et al., 1996; Boezio et al., 1997):

1. At least 12 (out of 18) position measurements in the x direction (direction of maximum bending) and 8 (out of 12) in the y direction were used in the fit.
2. There should be an acceptable chi-square for the fitted track in both directions with stronger requirements on the x -direction.

In addition to these conditions, we required that the deflections determined by the tracking information from only the top half, only the lower half and from the whole spectrometer should be consistent. This selection was used to remove scattered events and was imposed only on events below the antiproton threshold of the RICH. Above the RICH threshold, the mass resolution was sufficient to reject scattered protons from the \bar{p} sample. To remove the contamination from spillover protons in the antiproton sample, we required that the error on the deflection, estimated on an event-by-event basis during the fitting procedure (Golden et al., 1991), should be less than $0.008 (\text{GV})^{-1}$.

Downward moving particles were selected using the ToF information. The time-of-flight resolution of about 200 ps on a flight path of 1.2 m assured that no contamination from albedo particles remained in the selected sample. The ionization loss in the top ToF scintillator was used to select minimum ionizing singly charged particles.

The calorimeter was primarily used to reject electrons. The longitudinal and transverse segmentation of the calorimeter combined with the measurement of the energy lost by the particle in each silicon strip resulted in a high identification power for electromagnetic showers. Using simulated electrons and antiprotons and following the experience gained in the CAPRICE94 flight (Boezio et al., 1997), we defined an energy dependent calorimeter antiproton selection which rejected $(99.4 \pm 0.2)\%$ of the electrons, independent of rigidity in the interval from 4 to 50 GV. The antiproton selection efficiency was found varying slowly with rigidity decreasing from about 97% at 4 GV to about 92% above 30 GV.

The RICH was used to measure the Cherenkov angle of the particles and hence their velocities. Below the threshold rigidity for antiprotons to produce Cherenkov light in the gas (about 18 GV) the detector was used as a threshold device to veto lighter particles, while above it the Cherenkov angle was reconstructed. Below 25 GV the fluctuations in the number of detected photoelectrons were quite large due to variations in threshold rigidity caused by pressure variation in the radiating gas and because of large Poisson fluctuations as the average number of photoelectrons detected at this rigidity was 6. Therefore, antiprotons in the rigidity range 4 to 25 GV were selected if the event did not produce a Cherenkov signal or when the reconstructed Cherenkov angle was consistent with that of an antiproton with the measured rigidity.

The selection criteria imposed on the RICH data to select antiprotons were tested using both a sample of electrons selected by the calorimeter using the flight data and a sample of muons collected at ground prior to the launch. The fraction of muons surviving the antiproton RICH selection was $(0.36^{+0.13}_{-0.10})\%$ between 4 and 8 GV, $(0.30^{+0.18}_{-0.12})\%$ between 8 and 18 GV, $(0.76^{+0.60}_{-0.36})\%$ between 18 and 30 GV and $(1.7^{+1.4}_{-0.8})\%$ between 30 and 50 GV.

The fraction of muons surviving the antiproton RICH selection was $(0.22^{+0.07}_{-0.05})\%$ below 30 GV increasing to $(1.5^{+1.2}_{-0.7})\%$ between 30 and 50 GV. The fraction of electrons that survived the RICH antiproton criteria was $(0.20^{+0.47}_{-0.17})\%$, consistent with the level of contamination obtained from the ground muons.

Using the calorimeter and the RICH together the electron contamination in the antiproton sample was reduced to a negligible amount. The contamination due to muons was derived defining negative muons all the events surviving the tracking, ToF and calorimeter antiproton selection criteria and multiplying these numbers by the RICH muon contamination determined above. The muon contamination in the antiproton sample was estimated to be $1.1^{+0.4}_{-0.3}$ in the first rigidity bin, $0.28^{+0.17}_{-0.11}$ in the second, $0.15^{+0.12}_{-0.07}$ in the third and $0.10^{+0.15}_{-0.08}$ in the fourth. Then, this contamination was subtracted from the antiproton signal.

Contamination from spillover protons was studied using the actual flight data and was found to be negligible (Bergström, 2000).

4 Results

All antiprotons and protons interacting with the payload material above the tracking system were assumed to be rejected by the selection criteria. The data were corrected for these losses with multiplicative factors, using the expression for the interaction mean free path for the different materials in the detectors given by Stephens (1997).

For the atmospheric secondary antiproton production, we used the calculation by Stephens (1997) and for that of protons the data of Papini et al. (1996). The secondary produced particles were normalized with the acceptance and live time of the experiment, and subtracted from the corrected numbers using a mean residual atmosphere of 5.5 g/cm^2 . Then, the data were corrected for losses in the atmosphere above the detector due to interactions, giving the number of antiprotons and protons at the top of the atmosphere. The geometrical factor at different rigidities was obtained with a Monte Carlo technique. Finally, the transmission of the particles through the earth's magnetic field was taken into account with the usage of corrections factors. These factors differed from 1 only in the first rigidity interval.

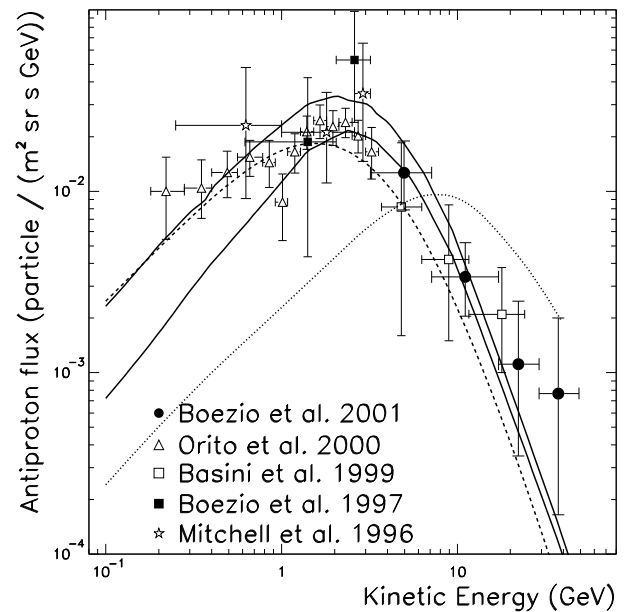


Fig. 2. The antiproton flux at the top of the atmosphere obtained in this work compared to other recent experiments and theoretical calculations.

Fig. 2 shows the antiproton flux measured by this experiment together with other recent experimental data (Mitchell et al., 1996; Boezio et al., 1997; Basini et al., 1999; Orito et al., 2000). The two solid lines show the upper and lower limit of a calculated flux of interstellar antiprotons by Simon et al. (1998) assuming a pure secondary production during the propagation of cosmic rays in the Galaxy and using a

recently measured proton and helium spectra (Menn et al., 1997). The dashed line shows the interstellar secondary antiproton flux calculated by L. Bergström & P. Ullio (1999, private communication). This calculation used the interstellar proton spectrum measured by the CAPRICE94 experiment (Boezio et al., 1999). The dotted line shows the primary antiproton flux by Ullio (1999), which included a Minimal Supersymmetric Standard Model with a contribution from an assumed Higgsino-like neutralino, with a mass of 964 GeV. The theoretical fluxes, but not the experimental values of the other experiments, were corrected for the solar modulation conditions corresponding to the CAPRICE98 flight using a spherically symmetric model (Gleeson & Axford, 1968) with a solar modulation parameter of $\Phi = 600$ MV.

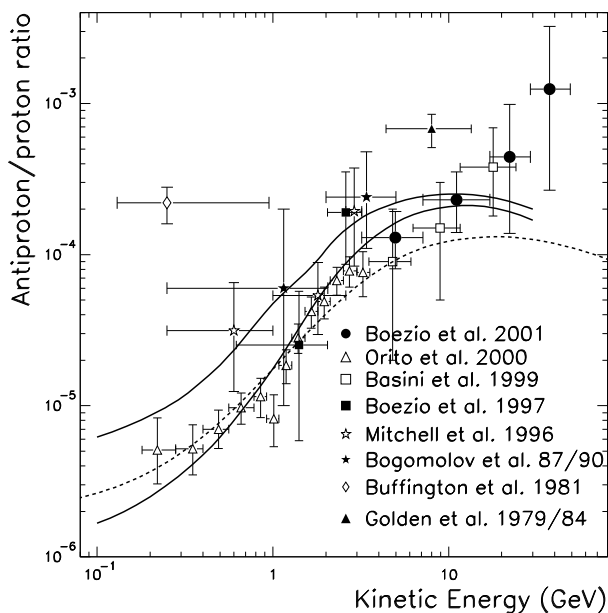


Fig. 3. The \bar{p}/p ratio at the top of the atmosphere obtained in this work compared to other recent experiments and theoretical calculations.

Fig. 3 shows the antiproton to proton ratio measured by CAPRICE98 along with other experimental data (Buffington et al., 1981; Golden et al., 1984; Bogomolov et al., 1987, 1990; Mitchell et al., 1996; Boezio et al., 1997; Basini et al., 1999; Orito et al., 2000) and with theoretical calculations. The two solid lines show the upper and lower limit of the calculated fraction of interstellar antiprotons by Simon et al. (1998). The dashed line shows the similar calculation by L. Bergström and P. Ullio (1999, private communication).

It is worth pointing out that to obtain the antiproton to proton ratio we did not correct for the selection efficiencies, which we considered to be the same for antiprotons and protons, hence, eliminating the systematic uncertainties related with the efficiencies estimations.

5 Conclusions

An electromagnetic calorimeter and a ring imaging Cherenkov detector were used to measure the cosmic ray flux of antiprotons. This combination made it possible to accurately identify antiprotons in the presence of a large background of lighter, negatively charge particles. It also allowed an accurate determination of the detector efficiencies as well as the contamination within the antiproton sample.

The antiproton flux and the antiproton to proton ratio have been determined in ~ 50 GeV wide energy region, more than a factor two larger than in previous experiments. Between 3 and 20 GeV our antiproton fluxes are consistent with the measurement by the MASS91 experiment (Hof et al., 1996) and, in the whole energy range, with the theoretical predictions by Simon et al. (1998) and L. Bergström and P. Ullio 1999 (private communication) which assume a purely secondary origin of the cosmic-ray antiprotons. However, a primary component cannot be excluded and the shape of the measured antiproton flux could indicate a presence of primary antiprotons.

References

- Ambriola, M. L. et al., Nucl. Phys. (Proc. Suppl.) B, 78, 32, 1999.
- Basini, G. et al., Proc. 26th ICRC, Salt Lake City 1999, 3, 77.
- Bergström, D., *Antiprotons in the cosmic radiation measured by the CAPRICE98 experiment*, PhD thesis, KTH Stockholm 2000, Sweden.
- Bergström, D. et al., to appear in Nucl. Instrum. Methods A., 2001.
- Bergström, L. et al., Phys. Rev. D, 59, 43506, 1999a.
- Bergström, L. et al., Astrophys. J., 526, 215, 1999b.
- Bocciolini, M. et al., Nucl. Instr. Meth. A, 370, 403, 1996; see also: Ricci, M. et al., Proc. 26th ICRC, Salt Lake City 1999, 5, 49.
- Boezio, M. et al., Astrophys. J., 487, 415, 1997.
- Boezio, M. et al., Astrophys. J., 518, 457, 1999.
- Bogomolov, E. A. et al., Proc. 20th ICRC, Moscow 1987, 2, 72; Bogomolov, E. A. et al., Proc. 21st ICRC, Adelaide 1990, 3, 288.
- Bottino, A. et al., Phys. Rev. D., 58, 123503, 1998.
- Buffington, A. et al., Astrophys. J., 248, 1179, 1981.
- Francke, T. et al., Nucl. Instrum. Methods, A433, 87, 1999.
- Gleeson, L. J. and Axford, W. I., Astrophys. J., 154, 1011, 1968.
- Golden, R. L. et al., Phys. Rev. Lett., 43, 1264, 1979.
- Golden, R. L. et al., Astrophys. Lett. 24, 75, 1984.
- Golden, R. L. et al., Nucl. Instrum. Methods, A306, 366, 1991.
- Hawking, S. W., Nature, 126, 30, 1974.
- Hof, M. et al., Nucl. Instr. and Meth., A345, 561, 1994.
- Hof, M. et al., Astrophys. J., 467, L33, 1996.
- Kiraly, P. et al., Nature, 293, 120, 1981.
- Maki, K. et al., Phys. Rev. Lett., 76, 3474, 1996.
- Menn, W. et al., Proc. 26th ICRC, Durban 1997, 3, 409.
- Mitchell, J. et al., Phys. Rev. Lett., 76, 3057, 1996.
- Orito, S. et al., Phys. Rev. Lett., 84, 1078, 2000.
- Papini, P. et al., Nuovo Cimento, 19, 367, 1996.
- Simon, M. et al., Astrophys. J., 499, 250, 1998.
- Stecker, F. W., Rudaz, S., and Walsh T. F., Phys. Rev. Lett., 55, 2622, 1985.
- Stephens, S. A., Astropart. Phys., 6, 229, 1997.
- Ullio, P. 1999, astro-ph/9904086